remote sensing

MDPI

Article

Validation of the Suomi NPP VIIRS Ice Surface Temperature Environmental Data Record

Yinghui Liu [1,*], Jeffrey Key [2], Mark Tschudi [3], Richard Dworak [1], Robert Mahoney [4] and Daniel Baldwin [3]

Received: 28 October 2015; Accepted: 11 December 2015; Published: 18 December 2015
Academic Editors: Changyong Cao, Magaly Koch and Prasad Thenkabail

1 Cooperative Institute for Meteorological Satellite Studies, University of Wisconsin-Madison, 1225 West Dayton St., Madison, WI 53706, USA; rdworak@ssec.wisc.edu
2 NOAA/NESDIS, 1225 West Dayton St., Madison, WI 53706, USA; jkey@ssec.wisc.edu
3 Colorado Center for Astrodynamics Research, University of Colorado, Boulder, CO 80309, USA; mark.tschudi@colorado.edu (M.T.); daniel.baldwin@colorado.edu (D.B.)
4 Northrop Grumman Aerospace Systems, Redondo Beach, CA 90278, USA; robert.mahoney@ngc.com
* Correspondence: yinghuil@ssec.wisc.edu; Tel.: +1-608-890-1893; Fax: +1-608-262-5974

Abstract: Continuous monitoring of the surface temperature is critical to understanding and forecasting Arctic climate change; as surface temperature integrates changes in the surface energy budget. The sea-ice surface temperature (IST) has been measured with optical and thermal infrared sensors for many years. With the IST Environmental Data Record (EDR) available from the Visible Infrared Imaging Radiometer Suite (VIIRS) onboard the Suomi National Polar-orbiting Partnership (NPP) and future Joint Polar Satellite System (JPSS) satellites; we can continue to monitor and investigate Arctic climate change. This work examines the quality of the VIIRS IST EDR. Validation is performed through comparisons with multiple datasets; including NASA IceBridge measurements; air temperature from Arctic drifting ice buoys; Moderate Resolution Imaging Spectroradiometer (MODIS) IST; MODIS IST simultaneous nadir overpass (SNO); and surface air temperature from the National Centers for Environmental Prediction/National Center for Atmospheric Research (NCEP/NCAR) reanalysis. Results show biases of −0.34; −0.12; 0.16; −3.20; and −3.41 K compared to an aircraft-mounted downward-looking pyrometer; MODIS; MODIS SNO; drifting buoy; and NCEP/NCAR reanalysis; respectively; root-mean-square errors of 0.98; 1.02; 0.95; 4.89; and 6.94 K; and root-mean-square errors with the bias removed of 0.92; 1.01; 0.94; 3.70; and 6.04 K. Based on the IceBridge and MODIS results; the VIIRS IST uncertainty (RMSE) meets or exceeds the JPSS system requirement of 1.0 K. The product can therefore be considered useful for meteorological and climatological applications.

Keywords: Suomi NPP; ice surface temperature; Environmental Data Record; calibration and validation

1. Introduction

The Arctic has been warming at a greater rate than anywhere else on Earth, a trend that is projected to continue over the next century [1]. Continuous measurements of the surface temperature are therefore important to the understanding, monitoring, and forecasting Arctic climate change. The surface temperature of sea ice, hereafter referred to as the "ice surface temperature (IST)", is the controlling factor for sea ice growth and melt. Furthermore, the strength of low-level atmospheric temperature inversions depends on the IST. IST and precipitable water are interdependent [2], as both the lower tropospheric temperature structure and water vapor content determine the downwelling longwave radiation. Consequently, changes in sea ice characteristics, temperature inversion strength,

precipitable water, and associated cloud cover all feed back to the surface temperature. Therefore, accurate and spatially robust surface temperature measurements are required to better understand feedbacks within the Arctic climate system and to better quantify the degree to which the Arctic is warming at a greater rate than the global average, known as "Arctic amplification" [3,4].

Satellite imagers with longwave infrared bands have been used to measure the ice surface temperature under clear conditions for many years. Key and Haefliger [5] presented an algorithm for estimating IST using split-window thermal channels at 11 and 12 μm of the Advanced Very High Resolution Radiometer (AVHRR) sensors. Key *et al.* [6] presented some improvements to the Key and Haefliger [5] procedure. The method was applied to a multi-decadal time series of AVHRR to study recent climate change in the Polar Regions [7–11]. Hall *et al.* [12] adopted the Key *et al.* [6] method for use with the Moderate-Resolution Imaging Spectroradiometer (MODIS) onboard the Terra and Aqua satellites. Their validation yielded a root mean square error (RMSE) of 1.2 K when compared to near-surface air temperature. Methods have also been developed for the estimation of land surface temperature from remotely sensed satellite-based thermal infrared data [13]. The accuracy of those retrievals has been assessed in a variety of validation studies [13–16].

IST is now produced with the Visible Infrared Imager Radiometer Suite (VIIRS) onboard the Suomi National Polar-orbiting Partnership (NPP) satellite. It is one of the official VIIRS products, or Environmental Data Records (EDR). VIIRS has some advantages over its heritage sensors [17] in that the split window bands at 11 and 12 μm in "moderate" resolution have higher spatial resolution than both AVHRR and MODIS, with approximately 1.6 km for VIIRS at the edge of the scan (750 m at nadir) compared to 4.8 km for MODIS (1 km at nadir). VIIRS also has a wider swath than MODIS, approximately 3000 km *versus* 2330 km. Figure 1 gives an example of a daily composite of the VIIRS IST EDR on 1 March 2015. It shows the lowest IST north of the Canadian Archipelago and Greenland, higher temperatures north of Alaska, and the warmest areas around the Kara Sea and Bering Strait.

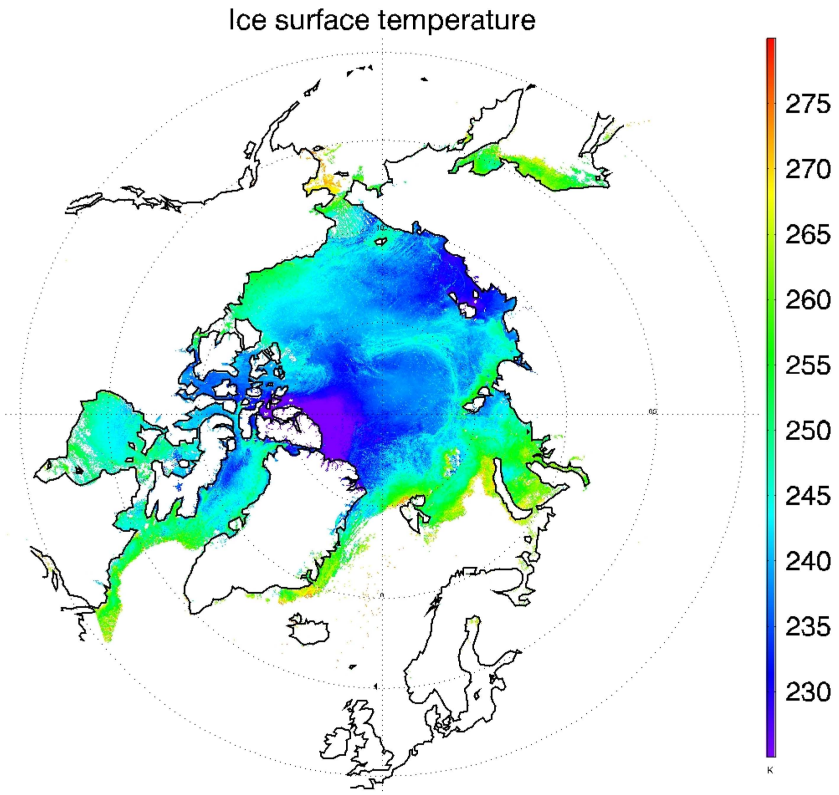

Figure 1. Ice surface temperature (IST) composite of the Visible Infrared Imaging Radiometer Suite (VIIRS) IST Environmental Data Record (EDR) from all overpasses over the Arctic on 1 March 2015.

This study presents the validation of the VIIRS IST EDR with multiple datasets, including aircraft measurements, 2 m air temperature from Arctic drifting buoys, MODIS IST, and surface air temperatures from an atmospheric reanalysis product. This work significantly extends the preliminary validation study of Key *et al.* [18] by employing additional IST product inter-comparisons, thereby providing a robust evaluation of the operational VIIRS IST product.

2. Data and Methods

The VIIRS IST EDR provides clear-sky surface skin temperature retrievals at VIIRS moderate resolution (750 m) for both day and night over snow and ice covered water surfaces. The VIIRS IST EDR algorithm is based on the split-window technique of Yu *et al.* [19]. This statistical regression method is implemented as:

$$\mathrm{IST} = a_0 + a_1 T_{11} + a_2 \left(T_{11} - T_{12}\right) + a_3 \left(\sec\left(z\right) - 1\right) \quad (1)$$

where T_{11} and T_{12} are the VIIRS brightness temperature at 10.8 μm and 12.0 μm in moderate resolution bands M15 and M16 respectively, z is the satellite zenith angle, and a_0, a_1, a_2, and a_3 are regression coefficients.

Different sets of coefficients are used for daytime and nighttime retrievals. Day is defined by solar zenith angles (SZA) less than 85 degrees. Retrievals are done only under clear sky conditions, which are identified with the VIIRS cloud mask [20]. The brightness temperature difference term in Equation (1) is for the correction of atmospheric water vapor absorption; the term that includes the satellite zenith angle accounts for the atmosphere path length. In this study, VIIRS IST EDR data produced by the Interface Data Processing Segment (IDPS) over the period August 2012 to July 2015 are used.

The algorithm described above is similar to the ice surface temperature algorithm first developed by Key and Haefliger [5] and later revised by Key *et al.* [6]. This approach is also similar to those used for sea surface temperature (SST) estimation. Other related algorithms are described by Comiso [21] and Lindsay and Rothrock [22].

The IDPS operational IST product [23] is based on prelaunch regression coefficients [24] derived from Global Synthetic Data [25,26] that includes the effects of VIIRS sensor relative spectral response and sensor noise, based on VIIRS F1 prelaunch, sensor characterization test measurements. At-sensor, clear sky, top-of-atmosphere (TOA) synthetic radiances for the VIIRS 10.8 μm and 12.0 μm IR bands were computed using the MODerate resolution atmospheric TRANsmission (MODTRAN) [27] radiative transfer model with inputs derived from physical properties based on NCEP Global Forecast System (GFS) snow/ice mask, surface skin-temperature and atmospheric data. VIIRS sensor effects were incorporated into the simulated radiances based on a VIIRS sensor model [28].

2.1. Validation Datasets

The datasets used to validate the VIIRS IST are summarized in Table 1. IST data sets from MODIS, specifically the Terra MODIS (MOD29) and Aqua MODIS (MYD29) Sea Ice Extent 5-Min L2 Swath 1 km datasets [29,30] from August 2012 to July 2015 are used to compare with the VIIIRS IST EDR. These data sets are in swath format at 1 km resolution at nadir for both daytime and nighttime under clear sky conditions, with swath coverage of 2330 km (cross track) by 2030 km (along track). To collocate the VIIRS IST EDR and MODIS IST, every overpass over the Arctic and Antarctic of the VIIRS IST EDR and MODIS IST are re-gridded to a 1 km Equal-Area Earth Grid (EASE-Grid), with 9025 by 9025 grid cells extending from 48.4 to 90°N over the Arctic and 8025 by 8025 grid cells extending from 53.2 to 90°S over the Antarctic. Only grids cells with VIIRS-MODIS observation time differences of less than 5 min, and indicated as cloud free from both VIIRS and MODIS cloud masks, are included in the matchup comparison.

Table 1. Validation datasets used in this study.

Validation Dataset	Parameter	Spatial Resolution	Spatial Coverage	Temporal Coverage
NASA IceBridge KT-19 IR Surface Temperature	Snow/ice temperature	15 × 15 m	Arctic and Antarctic	Arctic: 2012–2014 Antarctic: 2012–2013
MODIS Ice Surface Temperature	Snow/ice temperature	1 km	Arctic and Antarctic	August 2012–July 2015
MODIS simultaneous nadir overpass	Snow/ice temperature	0.05 degree longitude by 0.05 degree latitude	Arctic	March 2013–April 2014
Arctic drifting buoy	2 m air temperature	Point observations	Arctic	August 2012–June 2014
NCEP/NCAR reanalysis	Air temperature at 0.995 sigma level	2.5 × 2.5 degree latitude/longitude	Arctic and Antarctic	August 2012–July 2015

An additional comparison of VIIRS and MYD29 IST values based on S-NPP and Aqua Simultaneous Nadir Overpass (SNO) orbit swaths within a 5 min time window covering the Arctic is also performed. The matchup IST values for the SNO comparisons are binned and averaged to a 1/20th degree equal angle, Climate Model Grid (CMG). The SNO IST comparison matchups include only pixels indicated as confidently clear by the VIIRS cloud mask with satellite view zenith angles less than 45 degrees and ice concentrations greater than or equal to 95%, as estimated by the VIIRS Ice Concentration Intermediate Product (IP) [31]. For this comparison, 20 SNO orbit swaths from March 2013 to April 2014 are used, thus capturing a relatively broad range of temperatures.

IST measured with an airborne Heitronics KT-19.85 Series II infrared radiation pyrometer (KT-19) on a National Aeronautics and Space Administration (NASA) P3 during the NASA Operation IceBridge campaigns [32] is used to validate the VIIRS IST EDR. One of the NASA IceBridge mission goals is to better understand the processes that connect Polar Regions with the global climate system [33]. All KT-19 observations in the Antarctic in 2012 and 2013, and in the Arctic in 2014, are used to validate collocated VIIRS IST EDR. All available KT-19 temperature measurements that are within 375 m of the center of the VIIRS pixel are averaged. Only KT-19 temperature samples with standard deviations less than 1 K are used in matchup comparisons in order to eliminate cases with small-scale IST outliers that VIIRS would not be able to resolve. In addition, the closest KT-19 point to the VIIRS pixel must be within 15 min and 100 meters to be considered. Finally, a rigorous quality control is done to make sure that the VIIRS IST value is not contaminated by cloud.

If a daylight (SZA less than 85°) scene is used, a false-color image is created with VIIRS bands M5, M7, and M10 (0.67, 0.85, and 1.6 μm). These images are visually inspected to confirm that the daytime scene is clear sky. For the few available scenes that are night (SZA 90° or more), a visual inspection of the M15 and M16 (10.8, 12.0 μm) images is done. It should be noted that no cases with SZA between 80° and 90° are used in the statistics because of the large increase in random error observed in ice and cloud products for such low-sun conditions.

The NCEP/NCAR Reanalysis dataset [34] provides surface air temperature at the 0.995 sigma level from 1948 to the present. The daily surface air temperature data is available at 00Z, 06Z, 12Z, and 18Z with a spatial resolution of 2.5 × 2.5 degrees latitude/longitude. The following approach is used to match the NCEP/NCAR reanalysis surface temperature with VIIRST IST EDR. For each VIIRS IST EDR overpass, the IST values in the 1 km EASE-Grid projection are remapped to a 2.5 × 2.5 degree latitude/longitude grid. If the ratio of available remapped samples to the maximum possible sample number in a grid cell is larger than a threshold of 0.9, the mean of all the remapped VIIRS IST EDRs is assigned to that grid cell. Using the median of all the remapped VIIRS IST EDRs produces the same results, as shown in the following section.

Surface air temperatures (SAT) measured by drifting ice buoys from the International Arctic Buoy Programme (IABP) [35] are also used to assess the accuracy of the VIIRS IST EDR. Unfortunately, issues such as solar heating, frost and snow can lead to inaccurate SAT buoy measurements. Sensors

with the most accurate measurements are the 2 m, shielded thermistors (personal communication, I. Rigor, 2015). In this study, SAT measurements from four drifting buoys from August 2012 to June 2014 are used, with buoy IDs 300025010128510, 300025010125530, 300025010123530, and 300234011045700, which are all ice mass balance buoys. More details of these buoys are available at http://iabp.apl.washington.edu/maps_daily_table.html. To collocate the buoy SAT observations and the VIIRS IST EDR, both are remapped to 1 km EASE-Grid, and only cases of collocated buoy SAT measurements and the VIIRS IST EDR within 2 h of each other are included.

2.2. Definition of Statistics

In the following sections three quantities are used to quantify the differences between two datasets. The bias, $\overline{\epsilon}$, is the average difference between observations in two datasets:

$$\overline{\epsilon} = \frac{1}{n}\sum_{i=1}^{n} e_i \tag{2}$$

where e_i is the difference between individual observations in the two samples—the "errors"—and n is the sample size. The root mean square error (RMSE) is the square root of the mean squared difference between two datasets:

$$RMSE = \sqrt{\frac{1}{n-1}\sum_{i=1}^{n} e_i^2} \tag{3}$$

The RMSE with the bias removed is the square root of the average squared deviation of the errors from the mean error, which is the standard deviation of the errors:

$$RMSE_{nobias} = \sqrt{\frac{1}{n-1}\sum_{i=1}^{n} (e_i - \overline{\epsilon})^2} \tag{4}$$

For the JPSS program, the absolute value of the bias in Equation (2) is termed the measurement accuracy. RMSE in Equation (3) is the measurement uncertainty. The RMSE with the bias removed, or the standard deviation, in Equation (4) is the measurement precision. If the bias is zero, RMSE and $\text{RMSE}_{\text{nobias}}$ are equal.

3. IST Validation Results

3.1. Comparison with MODIS IST

The MODIS IST product has been validated with surface air temperatures from weather stations and from buoy air temperatures, with a reported RMSE in the range of 1.2–1.3 K [12]. The MODIS IST product has been used in climate-related studies [29,30]. Comparisons of VIIRS IST EDR with MODIS IST can therefore demonstrate both consistency and accuracy. Histograms of the differences between VIIRS IST and MODIS IST match-ups are shown in Figure 2 for all cases, and in Figure 3 for cases with MODIS IST in the ranges 213–230 K, 230–240 K, 240–250 K, 250–260 K, 260–270 K, and 270–275 K. For over 2 billion match-up pairs, the VIIRS IST EDR shows a bias of −0.12 K with MODIS IST, and the $\text{RMSE}_{\text{nobias}}$ of 1.01 K. The majority of the IST differences have absolute values less than 1 K. This shows that in general the VIIRS IST EDR can be considered to be as accurate as the MODIS IST product. The good agreement can be attributed to similar split-window retrieval approach of both products, and good quality clear/cloudy identification using both the VIIRS and MODIS cloud masks.

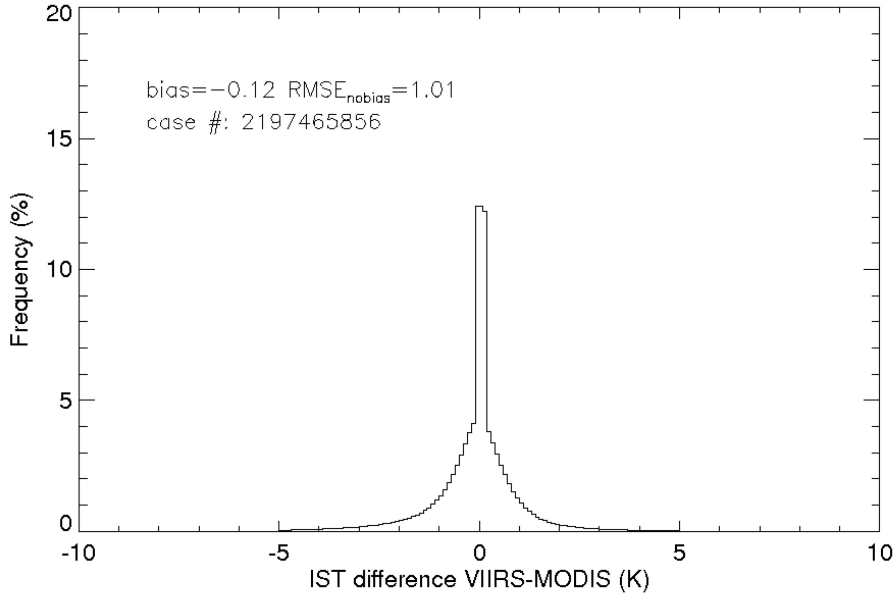

Figure 2. Histogram of ice surface temperature differences between Suomi National Polar-orbiting Partnership (S-NPP) VIIRS and MODIS (Aqua and Terra) in the Arctic and Antarctic for all cases from August 2012 to July 2015.

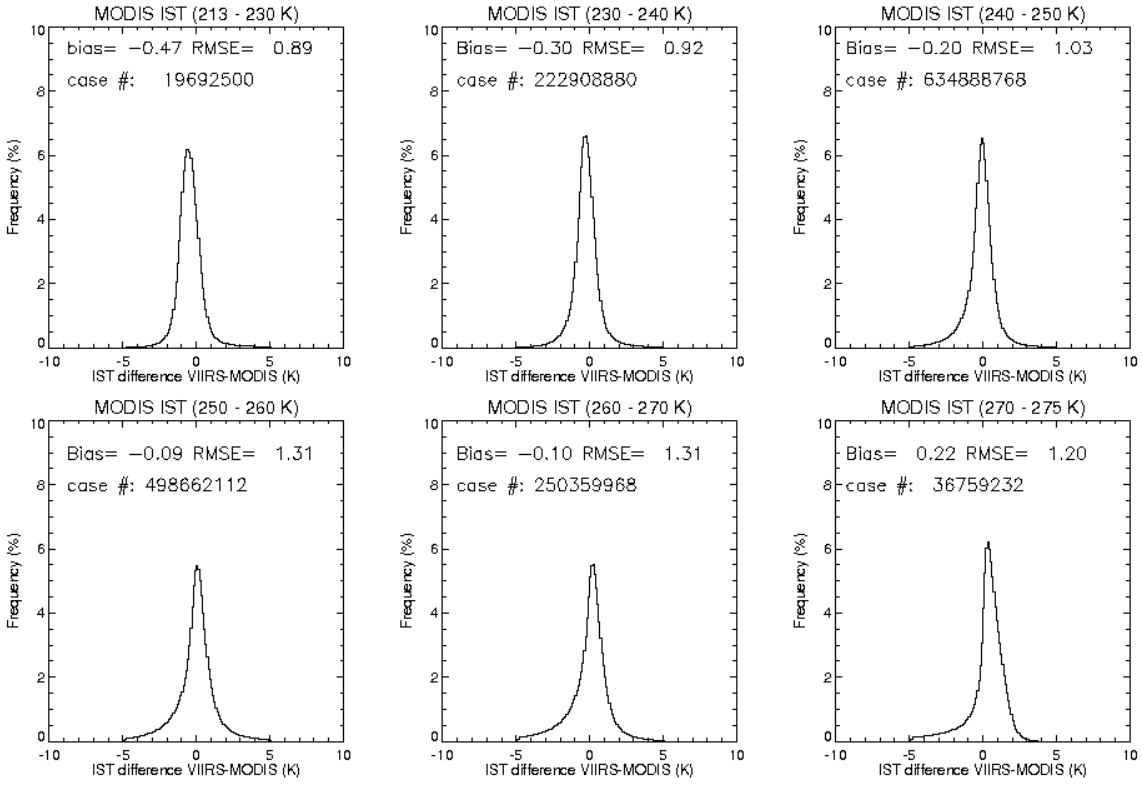

Figure 3. Histogram of ice surface temperature differences between NPP VIIRS and MODIS (Aqua and Terra) in the Arctic and Antarctic from August 2012 to July 2015 for cases with MODIS IST in the ranges 213–230 K, 230–240 K, 240–250 K, 250–260 K, 260–270 K, and 270–275 K. Measurement bias and $RMSE_{nobias}$ are indicated for each bin.

For the temperature bin with the MODIS IST between 270 and 275 K the bias is positive (0.22 K). The bias becomes negative (−0.10 K) for temperatures below 270 K, and becomes more negative

(−0.47) for temperatures less than 230 K. The $RMSE_{nobias}$ values are relatively stable, with smaller values for lower temperatures. RMSE is close to $RMSE_{nobias}$ because of the small bias, with RMSE of 1.02 K for all cases, and 1.00 K, 0.96 K, 1.05 K, 1.31 K, 1.31 K, and 1.22 K for MODIS IST in the ranges 213–230 K, 230–240 K, 240–250 K, 250–260 K, 260–270 K, and 270–275 K. The bias characteristics can be attributed to the differences between how the retrieval coefficients are derived for VIIRS and MODIS ISTs. For the VIIRS IST EDR, different sets of coefficients are used for daytime and nighttime. For MODIS, different retrieval coefficients are derived for three temperature ranges of the 11 μm brightness temperature: less than 240 K, 240–260 K, and greater than 260 K. Thus, the MODIS IST retrievals may benefit from this approach, and have a similar performance for all three temperature intervals. The VIIRS IST EDR thus tends to have close agreement with MODIS IST for the middle temperature range, and have a higher bias when temperatures are low or high.

Comparisons of VIIRS IST EDR and MODIS IST for the Arctic only are shown in Figures 4 and 5. The bias and $RMSE_{nobias}$ for all cases, and for different temperature bins, have similar values and characteristics as those from all cases in the Antarctic. The RMSE is close to $RMSE_{nobias}$ because of the small bias, with RMSE of 0.98 K for all cases, and 1.04 K, 0.88 K, 0.95 K, 1.25 K, 1.31 K, and 1.18 K for MODIS IST in the ranges 213–230 K, 230–240 K, 240–250 K, 250–260 K, 260–270 K, and 270–275 K. The more rigorous matchups of the VIIRS IST EDR and MODIS IST with SNO for the Arctic yield an absolute bias of 0.16 K, $RMSE_{nobias}$ of 0.94 K, and RMSE of 0.95 Ks. (Figure 6).

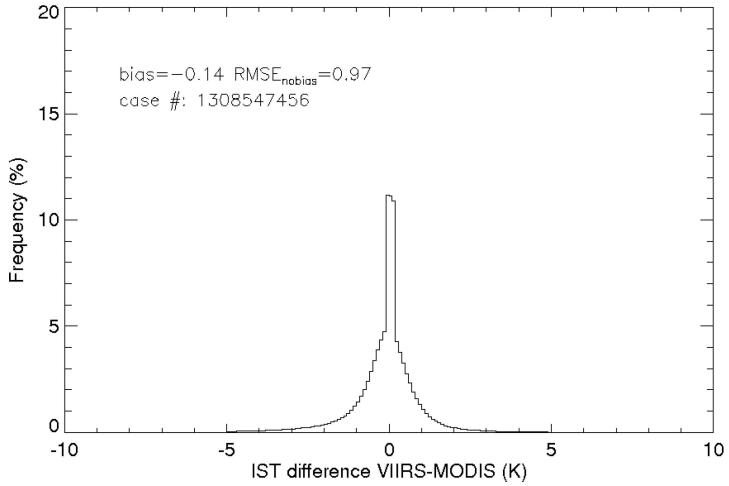

Figure 4. Histogram of ice surface temperature differences between NPP VIIRS and MODIS (Aqua and Terra) in the Arctic only for all cases from August 2012 to July 2015.

3.2. Validation with KT-19 IST

Though the inter-comparison of the VIIRS IST and the MODIS IST provides valuable information about the VIIRS IST EDR quality, the uncertainty of each needs to be determined with suitable "truth" data. The uncertainty in the MODIS IST has previously been evaluated with limited *in situ* validation [36]. The validation of the VIIRS IST EDR with KT-19 IST measurements provides the most accurate assessment of VIIRS IST EDR quality. The KT-19 sensor has been shown to accurately measure sea ice lead (fracture) temperatures of for leads 40 m wide or larger. With the rigorous procedures to collocate the KT-19 measurements with the VIIRS IST EDR, and with the elimination of the cloud contamination as detailed above, the comparison results give a high confidence assessment of the VIIRS IST EDR. With over 200 pairs of collocated VIIRS IST EDR and KT-19 IST over the Arctic and the Antarctic, the VIIRS minus KT-19 bias is −0.34 K, with an RMSE of 0.92 K (0.98 K) without (with) the bias included (Figure 7). With the bias removed, this RMSE is smaller than the 1.2–1.3 K value for the MODIS surface air temperature comparison in [12]. However, it should be noted that the IceBridge KT-19 measurements are concentrated in the springtime, when the surface temperatures are

in the moderate range and the VIIRS IST EDR performs best. More measurements from other seasons, when the IST is near the melting point or is very low, are desirable.

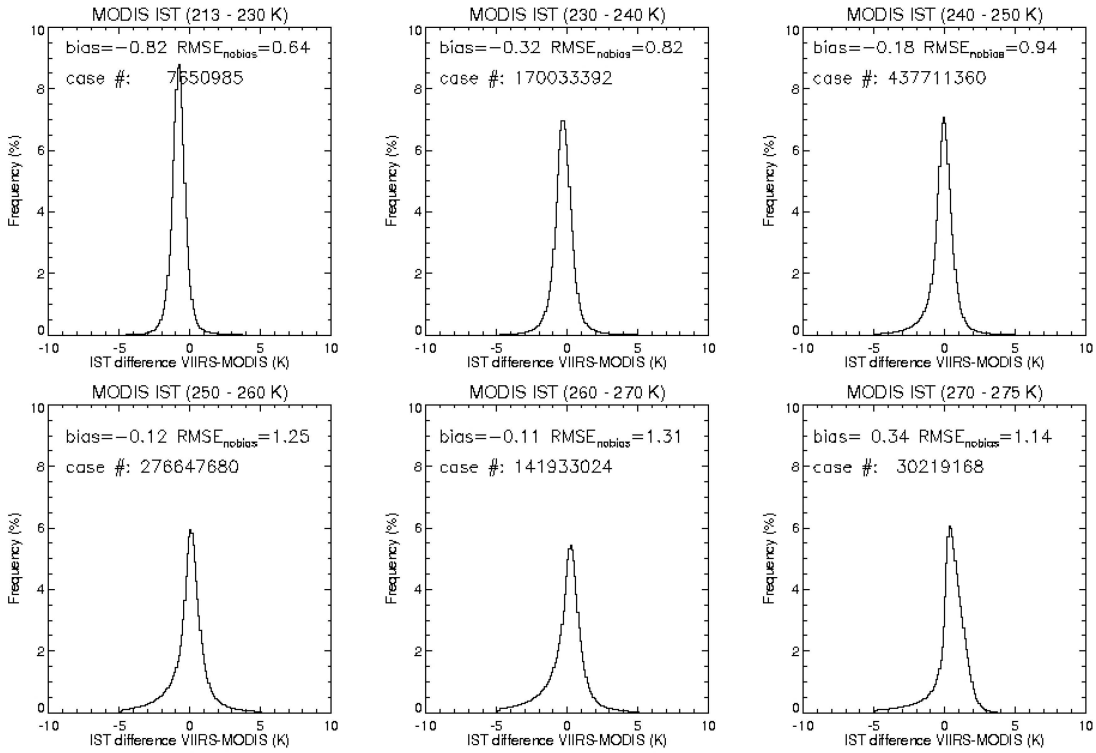

Figure 5. Histogram of ice surface temperature differences between NPP VIIRS and MODIS (Aqua and Terra) in the Arctic only from August 2012 to July 2015 for cases with MODIS ice surface temperature in the ranges 213–230 K, 230–240 K, 240–250 K, 250–260 K, 260–270 K, and 270–275 K. Measurement bias and $RMSE_{nobias}$ are indicated for each bin.

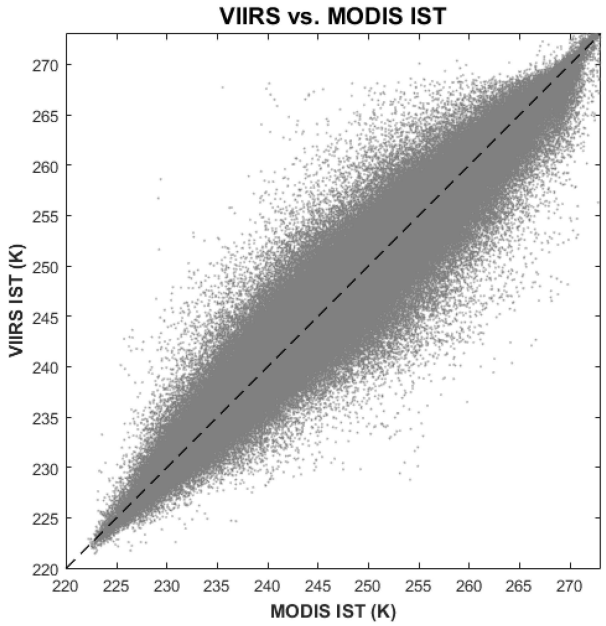

Figure 6. Scatter plot of IST from 20 NPP VIIRS and MODIS Aqua simultaneous nadir overpasses (SNO) over the Arctic from March 2013 to April 2014, with an overall bias of 0.16 K, $RMSE_{nobias}$ of 0.94 K, and RMSE of 0.95 K.

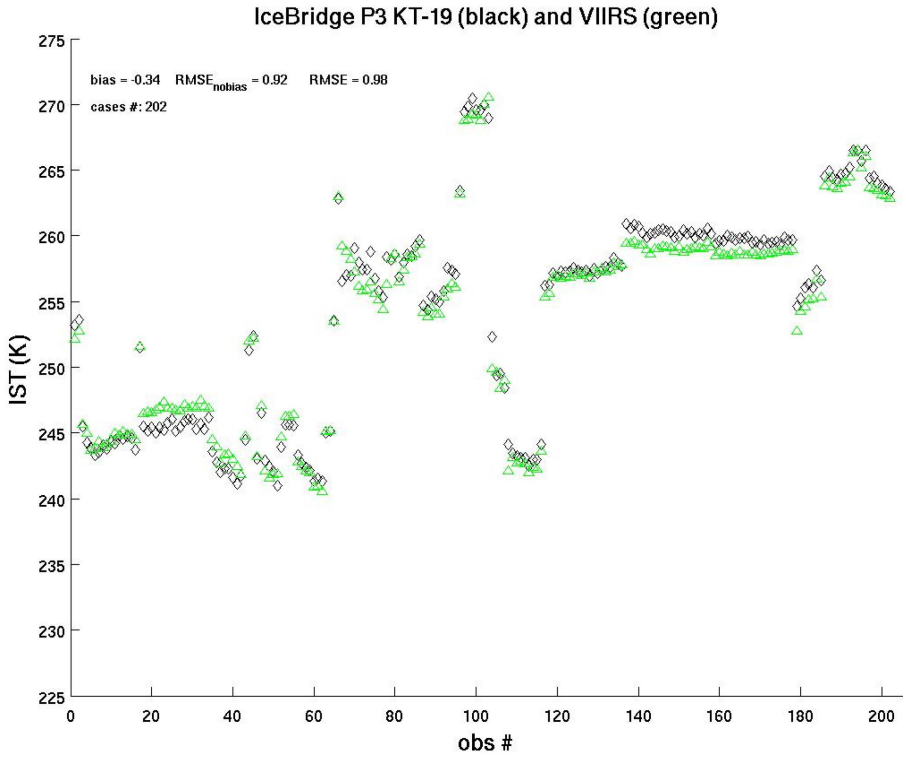

Figure 7. VIIRS IST (green) and KT-19 IST (black) for all coincident IceBridge flights with cloud-free observations over the Arctic (March–May 2014) and Antarctic (October–November 2012–2013).

3.3. Comparison with Drifting Buoy 2 m Air Temperature

The VIIRS IST EDR was also compared to the 2 m air temperature measured by drifting ice buoys in the Arctic (Figure 8). The results show a bias of −3.2 K, $RMSE_{nobias}$ of 3.7, and RMSE of 4.9 K, which means the VIIRS IST EDR is lower (colder) than the 2 m air temperature by over 3 K. The bias absolute values increase with increasing VIIRS IST.

3.4. Comparison with NCEP/NCAR Surface Air Temperature

Surface air temperature is assimilated in most of reanalyses and is also an output parameter [34,37]. However, the surface skin temperature over land and sea ice is not assimilated. The VIIRS IST EDR was compared to the surface air temperature from the NCEP/NCAR reanalysis [34]. Note that an additional comparison between the VIIRS IST and the NCEP-DOE Reanalysis 2 dataset [38] was also performed, but in our study the differences between the VIIRS IST and the NCEP/NCAR reanalysis were smaller than those from the VIIRS IST and NCEP-DOE comparisons. The results of the NCEP/NCAR comparison (Figures 9 and 10) show an overall bias of −3.41 K and an $RMSE_{nobias}$ of 6.04 K, so the VIIRS IST EDR is 3.41 K lower (colder) than the surface air temperature from the NCEP/NCAR reanalysis. On average, the $RMSE_{nobias}$ is larger than that of the drifting ice buoy comparison. The VIIRS IST has a minimum cold bias and $RMSE_{nobias}$ when VIIRS IST is between 270 and 275 K, opposite to the results from the comparison with drifting ice buoys. This cold bias generally increases with decreasing IST except for the IST range between 260 and 270 K. The maximum cold bias and $RMSE_{nobias}$ occur for IST between 213 and 230 K. The RMSE is 6.94 K for all cases, and 9.34 K, 7.35 K, 6.83 K, 6.87 K, 6.25 K, and 3.01 K for NCEP/NCAR surface air temperature in the ranges 213–230 K, 230–240 K, 240–250 K, 250–260 K, 260–270 K, and 270–275 K.

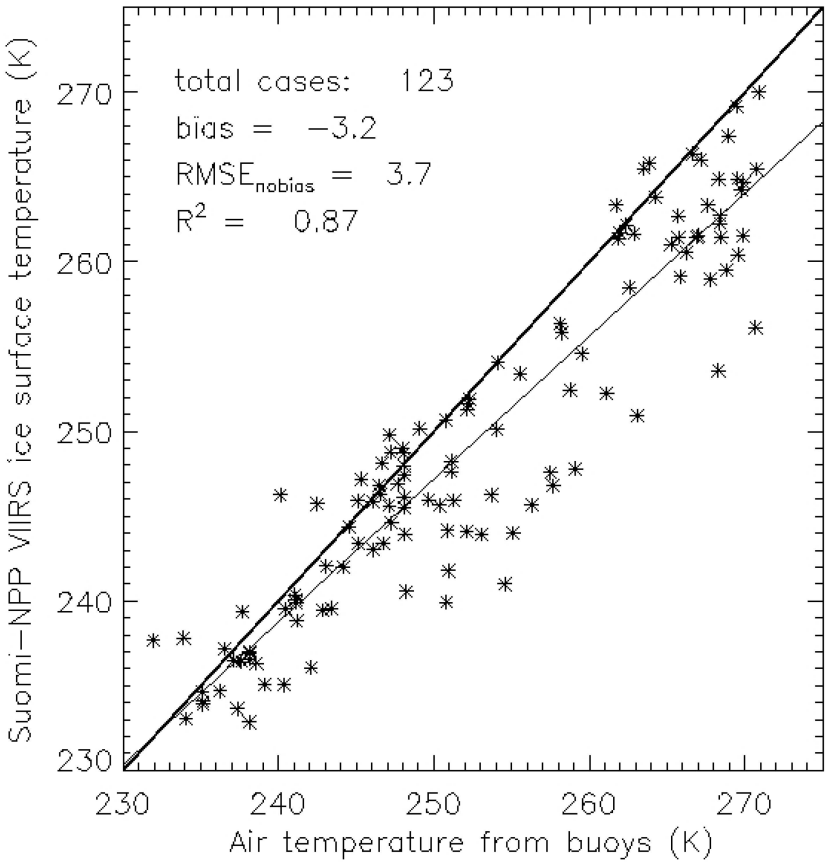

Figure 8. Scatterplot of surface air temperature from Arctic drifting ice buoys and VIIRS IST from August 2012 to June 2014. The thick line is the 1-to-1 ratio line; the thin line as the linear regression.

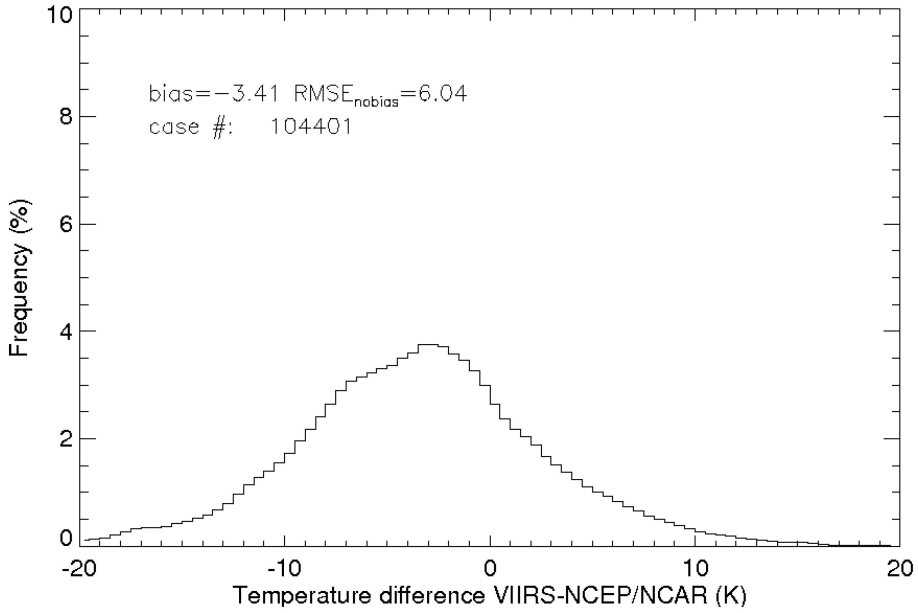

Figure 9. Histogram of ice surface temperature differences between VIIRS IST and National Centers for Environmental Prediction/National Center for Atmospheric Research (NCEP/NCAR) surface air temperature in the Arctic for all cases from August 2012 to July 2015.

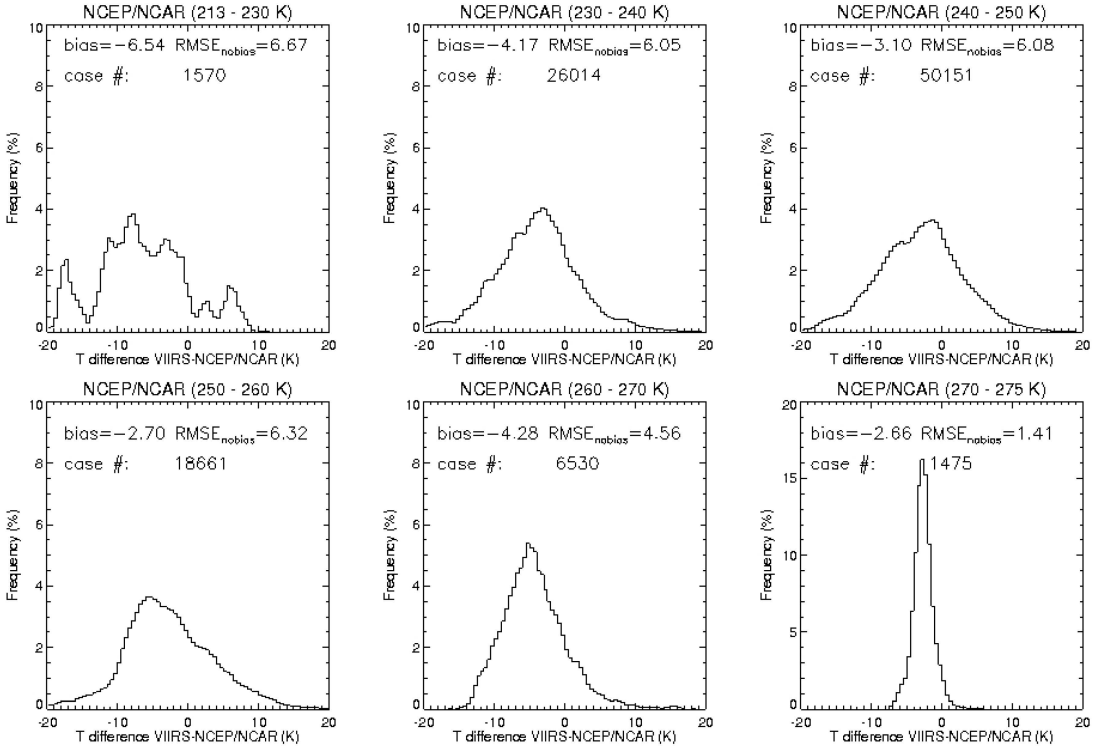

Figure 10. Histogram of ice surface temperature differences between VIIRS IST and NCEP/NCAR surface air temperature in the Arctic from August 2012 to July 2015 for cases with NCEP/NCAR surface air temperature in the ranges 213–230 K, 230–240 K, 240–250 K, 250–260 K, 260–270 K, and 270–275 K. Measurement bias and $RMSE_{nobias}$ are indicated for each bin.

Radionov *et al.* [39] showed that the average difference between the snow surface temperature and the 2 m air temperature is −0.7 K (surface is colder) during the June–August warm season, and −0.6 K in cold season from October to May. The annual mean difference in their measurements was −0.1 K. The largest differences are between −4.5 and −6.9 K from November to May, usually under clear sky conditions, and +2.1 to +5.5 in the warmer part of the year. Given that the VIIRS IST EDR is for clear-sky conditions only, differences larger than the averages reported in the Radionov *et al.*, study would be expected. Nevertheless, with thousands of cases in the comparisons of VIIRS, buoy, and reanalysis temperatures, a VIIRS cold bias of over 3 K may not be solely the result of air-skin temperature differences.

The large VIIRS IST cold bias, or reanalysis and buoy warm bias, may also be attributable to differences in the spatial coverage of VIIRS, drifting buoys, and the NCEP/NCAR reanalysis, and therefore the heterogeneity of the observed IST field. Due to the coarser resolution, the reanalysis is unable to resolve some of the complex IST features. The reanalysis could be smoothing out extreme values caused by features such as leads and polynyas that create small-scale temperature variations. A factor that could also explain the bias with drifting buoys is that some drifting buoys experience heating from sunlight, and as a result their temperatures may be biased high (warm). This would also cause a warm bias in the reanalysis, as buoy temperatures and pressures are assimilated [34]. Another third possibility is that cloud contamination, especially from high cirrus clouds, results in a low retrieved VIIRS IST.

4. Summary and Conclusions

Monitoring the surface temperature is important for climate studies globally, but it deserves special attention in the Polar Regions because of sparse surface observations, an extreme temperature range, and the unique surface and atmospheric characteristics. The VIIRS sensor onboard the

Suomi NPP and future Joint Polar Satellite System (JPSS) satellites provides an IST product with higher spatial resolution and wider coverage than heritage sensors such as AVHRR and MODIS with excellent radiometric quality. This study provided an assessment of the VIIRS IST EDR accuracy through comparisons with *in situ* and aircraft measurements, another satellite product, and a climate reanalysis.

Validation with KT-19 IST measurements from NASA Operation IceBridge flights over the Arctic and Antarctic in 2012–2014 yields a VIIRS IST cold bias of −0.34 K and an $RMSE_{nobias}$ of 0.92 K. An intercomparison with MODIS IST from 2012 to 2015 gives a VIIRS IST bias of −0.12 K and $RMSE_{nobias}$ of 1.01 K. The bias and $RMSE_{nobias}$ values show a dependence on temperature, with a positive bias for the warmer part of the range (270–275 K) and negative biases for lower temperatures. However, the bias and $RMSE_{nobias}$ values are relatively small in all temperature bins. A more rigorous simultaneous nadir overpass comparison shows an absolute bias of 0.16 K and an $RMSE_{nobias}$ of 0.94 K.

Comparisons of the VIIRS IST with 2 m air temperatures show a larger cold bias. Validation with drifting ice buoy 2 m air temperature yields a VIIRS IST bias of −3.2 K and $RMSE_{nobias}$ of 3.7 K. Comparisons to NCEP/NCAR Reanalysis surface air temperature produce a similar bias of −3.41 K and $RMSE_{nobias}$ of 6.04 K.

These validation and evaluation results demonstrate the high quality of the VIIRS IST EDR as indicated by the absolute bias and RMSE values for the IceBridge KT-19 measurement comparisons, where the KT-19 provide the best "truth" data for skin temperature. The results also show that the science quality of the VIIRS IST is similar to that of the MODIS IST. Based on the IceBridge and MODIS results, the VIIRS IST uncertainty (RMSE) meets or exceeds the JPSS system requirement of 1.0 K. The product can therefore be considered useful for meteorological and climatological applications. Furthermore, while we are not aware of any numerical weather prediction centers or climate reanalysis projects that assimilate satellite-derived ice surface temperature, the demonstrated accuracy of the IST product and the relatively large difference found in the comparison with the reanalysis surface temperatures provide motivation for research into its use in numerical models.

Acknowledgments: This work was supported by the Joint Polar Satellite System (JPSS) Program Office. MODIS ice surface temperature data is from the NASA Earth Observing System Data and Information System (EOSDIS) and the National Snow and Ice Data Center DAAC. NCEP Reanalysis data was provided by NOAA/OAR/ESRL PSD, Boulder, Colorado, USA, from their website at http://www.esrl.noaa.gov/psd/. The drifting buoy observations are from the International Arctic Buoy Programme, University of Washington at http://iabp.apl.washington.edu/index.html. KT-19 data is from the National Snow and Ice Data Center at http://nsidc.org/data/iakst1b. The VIIRS ice surface temperature data is from the JPSS Government Resources for Algorithm Verification, Independent Test and Evaluation (GRAVITE) system. The views, opinions, and findings contained in this report are those of the author(s) and should not be construed as an official National Oceanic and Atmospheric Administration or U.S. Government position, policy, or decision.

Author Contributions: Yinghui Liu designed the research, collected most of the data, carried out most of the data analysis, and wrote the manuscript. Jeffrey Key advised the whole study from the research method to the implementation, and has the greatest contribution on the revisions of the manuscript. Mark Tschudi introduced the KT-19 data, and did the initial analysis with Daniel Baldwin. Richard Dworak collected all the KT-19 data, and did the comparison of KT-19 with VIIRS IST EDR. Robert Mahoney did the VIIRS and MODIS Simultaneous Nadir Overpass analysis. All the authors contributed to the revisions of the manuscript.

Conflicts of Interest: The authors declare no conflict of interest.

References

1. IPCC. *Climate Change 2014: Impacts, Adaptation, and Vulnerability. Part B: Regional Aspects. Contribution of Working Group II to the Fifth Assessment Report of the Intergovernmental Panel on Climate Change*; Barros, V.R., Field, C.B., Dokken, D.J., Mastrandrea, M.D., Mach, K.J., Bilir, T.E., Chatterjee, M., Ebi, K.L., Estrada, Y.O., Genova, R.C., *et al*, Eds.; Cambridge University Press: Cambridge, UK; New York, NY, USA, 2014; p. 688.
2. Francis, J.A.; White, D.M.; Cassano, J.J.; Gutowski, W.J., Jr.; Hinzman, L.D.; Holland, M.M.; Steele, M.A.; Voeroesmarty, C.J. An arctic hydrologic system in transition: Feedbacks and impacts on terrestrial, marine, and human life. *J. Geophys. Res. Biogeosci.* **2009**, *114*. [CrossRef]

3. Solomon, S.; Qin, D.; Manning, M.; Chen, Z.; Marquis, M.; Averyt, K.B.; Tignor, M.; Miller, H.L.; IPCC. Summary for policymakers. In *Climate Change 2007: The Physical Science Basis*; Technical Report, Contribution of Working Group I, II and III to the Fourth Assessment Report of the Intergovernmental Panel on Climate Change; Cambridge University Press: Cambridge, UK; New York, NY, USA, 2007; p. 22.
4. Holland, M.M.; Bitz, C.M. Polar amplification of climate change in coupled models. *Clim. Dyn.* **2003**, *21*, 221–232. [CrossRef]
5. Key, J.; Haefliger, M. Arctic ice surface-temperature retrieval from AVHRR thermal channels. *J. Geophys. Res. Atmos.* **1992**, *97*, 5885–5893. [CrossRef]
6. Key, J.R.; Collins, J.B.; Fowler, C.; Stone, R.S. High-latitude surface temperature estimates from thermal satellite data. *Remote Sens. Environ.* **1997**, *61*, 302–309. [CrossRef]
7. Wang, X.; Key, J.R. Recent trends in arctic surface, cloud, and radiation properties from space. *Science* **2003**, *299*, 1725–1728. [CrossRef] [PubMed]
8. Wang, X.; Key, J.R. Arctic surface, cloud, and radiation properties based on the AVHRR polar pathfinder dataset. Part I: Spatial and temporal characteristics. *J. Clim.* **2005**, *18*, 2558–2574. [CrossRef]
9. Wang, X.; Key, J.R. Arctic surface, cloud, and radiation properties based on the AVHRR polar pathfinder dataset. Part II: Recent trends. *J. Clim.* **2005**, *18*, 2575–2593. [CrossRef]
10. Liu, Y.; Key, J.; Wang, X. Influence of changes in sea ice concentration and cloud cover on recent arctic surface temperature trends. *Geophys. Res. Lett.* **2009**, *36*. [CrossRef]
11. Liu, Y.; Key, J.; Wang, X. The influence of changes in cloud cover on recent surface temperature trends in the arctic. *J. Clim.* **2008**, *21*, 705–715. [CrossRef]
12. Hall, D.K.; Key, J.R.; Casey, K.A.; Riggs, G.A.; Cavalieri, D.J. Sea ice surface temperature product from MODIS. *IEEE Trans. Geosci. Remote Sens.* **2004**, *42*, 1076–1087. [CrossRef]
13. Duan, S.-B.; Li, Z.-L. Intercomparison of operational land surface temperature products derived from MSG-SEVIRI and Terra/Aqua-MODIS data. *IEEE J. Sel. Top. Appl. Earth Observ. Remote Sens.* **2015**, *8*, 4163–4170. [CrossRef]
14. Guillevic, P.C.; Privette, J.L.; Coudert, B.; Palecki, M.A.; Demarty, J.; Ottle, C.; Augustine, J.A. Land surface temperature product validation using NOAA's surface climate observation networks-scaling methodology for the visible infrared imager radiometer suite (VIIRS). *Remote Sens. Environ.* **2012**, *124*, 282–298. [CrossRef]
15. Wan, Z.; Li, Z.L. Radiance-based validation of the v5 MODIS land-surface temperature product. *Int. J. Remote Sens.* **2008**, *29*, 5373–5395. [CrossRef]
16. Li, Z.L.; Tang, B.H.; Wu, H.; Ren, H.; Yan, G.; Wan, Z.; Trigo, I.F.; Sobrino, J.A. Satellite-derived land surface temperature: Current status and perspectives. *Remote Sens. Environ.* **2013**, *131*, 14–37. [CrossRef]
17. Cao, C.; Xiong, J.; Blonski, S.; Liu, Q.; Uprety, S.; Xi, S.; Yan, B.; Weng, F. Suomi NPP VIIRS sensor data record verification, validation, and long-term performance monitoring. *J. Geophys. Res. Atmos.* **2013**, *118*, 664–678. [CrossRef]
18. Key, J.R.; Mahoney, R.; Liu, Y.; Romanov, P.; Tschudi, M.; Appel, I.; Maslanik, J.; Baldwin, D.; Wang, X.; Meade, P. Snow and ice products from Suomi NPP VIIRS. *J. Geophys. Res. Atmos.* **2013**, *118*, 12816–12830. [CrossRef]
19. Yu, Y.; Rothrock, D.A.; Lindsay, R.W. Accuracy of sea-ice temperature derived from the advanced very high-resolution radiometer. *J. Geophys. Res.: Oceans* **1995**, *100*, 4525–4532. [CrossRef]
20. Hutchison, K.D.; Roskovensky, J.K.; Jackson, J.M.; Heidinger, A.K.; Kopp, T.J.; Pavolonis, M.J.; Frey, R. Automated cloud detection and classification of data collected by the visible infrared imager radiometer suite (VIIRS). *Int. J. Remote Sens.* **2005**, *26*, 4681–4706. [CrossRef]
21. Comiso, J.C. Surface temperatures in the polar-regions from Nimbus-7 temperature humidity infrared radiometer. *J. Geophys. Res.: Oceans* **1994**, *99*, 5181–5200. [CrossRef]
22. Lindsay, R.W.; Rothrock, D.A. Arctic sea-ice surface-temperature from AVHRR. *J. Clim.* **1994**, *7*, 174–183. [CrossRef]
23. Baker, N. Joint Polar Satellite System (JPSS) VIIRS Ice Surface Temperature Algorithm Theoretical Basis Document Rev-A. Available online: http://npp.gsfc.nasa.gov/sciencedocs/2015-06/474-00052_ATBD-VIIRS-IST_A.pdf (accessed on 1 May 2013).

24. Ip, J.; Hauss, B. Pre-launch performance assessment of the VIIRS ice surface temperature algorithm. In Proceedings of the Fifth Annual Symposium on Future Operational Environmental Satellite Systems-NPOESS and GOES-R; 16th Conference on Satellite Meteorology and Oceanography; 89th Annual Meeting of the American Meteorological Society 89th, Phoenix, AZ, USA, 11–15 January 2009.
25. Baker, N. Joint Polar Satellite System (JPSS) NPP Operational Algorithm Proxy and Synthetic Test Data Description. Available online: http://www.star.nesdis.noaa.gov/jpss/documents/OAD/GSFC_474-00096_JPSS_NPP_Operational_Algorithm_Proxy_and_Synthetic_Test_Data__Alt._doc._no._D45702_.pdf (accessed on 3 January 2012).
26. Shoucri, M.; Hauss, B. Everest: An end-to-end simulation for assessing the performance of weather data products produced by environmental satellite systems. *Proc. SPIE* **2009**, *7458*, 74580G.
27. Berk, A.; Anderson, G.P.; Acharya, P.K.; Bernstein, L.S.; Muratov, L.; Lee, J.; Fox, M.; Adler-Golden, S.M.; Chetwynd, J.H.; Hoke, M.L. MODTRAN5: 2006 Update. *Proc. SPIE* **2006**, *6233*, 62331F.
28. Mills, S. Simulation and test of the VIIRS Sensor Data Record (SDR) algorithm for NPOESS. In Proceedings of the Third Symposium on Future National Operational Environmental Satellites; 87th AMS Annual Meeting, San Antonio, TX, USA, 13–18 January 2007.
29. Hall, D.K.; Riggs, G. *MODIS/Terra Sea Ice Extent 5-Min L2 Swath 1km, Version 6*; NASA National Snow and Ice Data Center Distributed Active Archive Center: Boulder, CO, USA, 2015.
30. Hall, D.K.; Riggs, G.A. *MODIS/Aqua Sea Ice Extent 5-Min L2 Swath 1 km, Version 6*; NASA National Snow and Ice Data Center Distributed Active Archive Center: Boulder, CO, USA, 2015.
31. Baker, N. Joint Polar Satellite System (JPSS) Operational Algorithm Description (OAD) for VIIRS Sea Ice Concentration Intermediate Product (IP) Software. Available online: http://npp.gsfc.nasa.gov/sciencedocs/2015-06/474-00094_OAD-VIIRS-SIC-IP_B.pdf (accessed on 3 June 2013).
32. Krabill, W.B.; Buzay, E. *IceBridge KT-19 IR Surface Temperature, Version 1. (2012–2015)*; Updated 2014; NASA National Snow and Ice Data Center Distributed Active Archive Center: Boulder, CO, USA, 2012.
33. Studinger, M.; Koenig, L.; Martin, S.; Sonntag, J. Operation IceBridge: Using instrumented aircraft to bridge the observational gap between icesat and ICESat-2. In Proceedings of 2010 IEEE International, Geoscience and Remote Sensing Symposium (IGARSS), Honolulu, HI, USA; 2010; pp. 1918–1919.
34. Kalnay, E.; Kanamitsu, M.; Kistler, R.; Collins, W.; Deaven, D.; Gandin, L.; Iredell, M.; Saha, S.; White, G.; Woollen, J.; *et al*. The NCEP/NCAR 40-year reanalysis project. *Bull. Am. Meteorol. Soc.* **1996**, *77*, 437–471. [CrossRef]
35. Rigor, I.G.; Colony, R.L.; Martin, S. Variations in surface air temperature observations in the arctic, 1979–1997. *J. Clim.* **2000**, *13*, 896–914. [CrossRef]
36. Scambos, T.A.; Haran, T.M.; Massom, R. Validation of AVHRR and MODIS ice surface temperature products using *in situ* radiometers. *Ann. Glaciol.* **2006**, *44*, 345–351. [CrossRef]
37. Dee, D.P.; Uppala, S.M.; Simmons, A.J.; Berrisford, P.; Poli, P.; Kobayashi, S.; Andrae, U.; Balmaseda, M.A.; Balsamo, G.; Bauer, P.; *et al*. The ERA-Interim reanalysis: Configuration and performance of the data assimilation system. *Q. J. R. Meteorol. Soc.* **2011**, *137*, 553–597. [CrossRef]
38. Kanamitsu, M.; Ebisuzaki, W.; Woollen, J.; Yang, S.K.; Hnilo, J.J.; Fiorino, M.; Potter, G.L. NCEP-DOE AMIP-II reanalysis (R-2). *Bull. Am. Meteorol. Soc.* **2002**, *83*, 1631–1643. [CrossRef]
39. Radionov, V.F.; Bryazgin, N.N.; Alexandrov, E.I. *The Snow Cover of the Arctic Basin*; Technical Report, APL-UW TR 9701; Applied Physics Laboratory, University of Washington: Seattle, WA, USA, 1997.